

# Collective density wave excitations in two-leg $\text{Sr}_{14-x}\text{Ca}_x\text{Cu}_{24}\text{O}_{41}$ ladders

A. Gozar<sup>1,2</sup>, G. Blumberg<sup>1,†</sup>, P. B. Littlewood<sup>3</sup>, B.S. Dennis<sup>1</sup>, N. Motoyama<sup>4</sup>, H. Eisaki<sup>5</sup>, and S. Uchida<sup>4</sup>

<sup>1</sup>*Bell Laboratories, Lucent Technologies, Murray Hill, NJ 07974*

<sup>2</sup>*University of Illinois at Urbana-Champaign, Urbana, IL 61801-3080*

<sup>3</sup>*University of Cambridge, Cavendish Laboratory, Cambridge, CB3 0HE UK*

<sup>4</sup>*The University of Tokyo, Bunkyo-ku, Tokyo 113, Japan*

<sup>5</sup>*Stanford University, Stanford, CA 94305*

(November 1, 2018)

Raman measurements in the  $1.5 - 20 \text{ cm}^{-1}$  energy range were performed on single crystals of  $\text{Sr}_{14-x}\text{Ca}_x\text{Cu}_{24}\text{O}_{41}$ . A quasielastic scattering peak (QEP) which softens with cooling is observed in the polarization parallel to the ladder direction for samples with  $x = 0, 8$  and  $12$ . The QEP is a Raman fingerprint of pinned collective density wave excitations screened by uncondensed carriers. Our results suggest that transport in metallic samples, which is similar to transport in underdoped high- $T_c$  cuprates, is driven by a collective electronic response.

PACS numbers: 78.30.-j, 71.27.+a, 71.45.-d

Competing ground states in low dimensional doped Mott-Hubbard systems have been the subject of extensive research in recent years [1]. Two-leg Cu-O based ladder materials like  $\text{Sr}_{14-x}\text{Ca}_x\text{Cu}_{24}\text{O}_{41}$  provide the opportunity to study not only magnetism in quasi one-dimensional (1D) quantum systems but also charge carrier dynamics in an antiferromagnetic environment, with relevance to the phase diagram of high- $T_c$  cuprates [2]. Magnetic correlations which give rise to a finite spin gap were predicted to generate an attractive interaction between doped carriers leading to superconductivity with a  $d$ -wave like order parameter. Due to the quasi-1D nature of these systems, ground states with broken translational symmetry in which single holes or hole pairs can order in a crystalline pattern are also possible. The balance between superconducting and spin/charge density wave (DW) ground states is ultimately determined by the microscopic parameters of the theoretical models [3].

The single crystals of  $\text{Sr}_{14-x}\text{Ca}_x\text{Cu}_{24}\text{O}_{41}$  contain quasi-1D two-leg  $\text{Cu}_2\text{O}_3$  ladder planes which are stacked alternately with planes of  $\text{CuO}_2$  chains along the  $b$  crystallographic axis [4]. The ladder direction defines the  $c$  axis and the lattice constants of these two sub-systems satisfy  $10c_{\text{chain}} \approx 7c_{\text{ladder}}$ . The nominal Cu valence in  $\text{Sr}_{14-x}\text{Ca}_x\text{Cu}_{24}\text{O}_{41}$  is  $+2.25$ , independent of Ca concentration. In the insulating  $\text{Sr}_{14}\text{Cu}_{24}\text{O}_{41}$  crystals most of the carriers are believed to be confined in the chains. Transport and optical conductivity data suggest that Ca substitution induces a transfer of holes from the chains to the more conductive ladders [5,6]. The ladder carrier density was estimated from the optical spectral weight to increase from  $0.07$  for  $x = 0$  to about  $0.2$  for  $x = 11$   $\text{Sr}_{14-x}\text{Ca}_x\text{Cu}_{24}\text{O}_{41}$  [6]. A crossover to metallic conduction at high temperatures takes place around  $x = 11$  [7] and for  $x = 12$  the  $c$ -axis  $dc$  resistivity has a minimum around  $T = 70 \text{ K}$  separating quasi-linear metallic and insulating behavior similar to the case of high- $T_c$  cuprates in the underdoped regime [8–10]. As opposed to  $\text{Sr}_{14-x}\text{Ca}_x\text{Cu}_{24}\text{O}_{41}$ , the isostructural com-

pound  $\text{La}_6\text{Ca}_8\text{Cu}_{24}\text{O}_{41}$  contains no holes per formula unit. At high Ca concentrations superconductivity under pressure has been observed in  $\text{Sr}_{14-x}\text{Ca}_x\text{Cu}_{24}\text{O}_{41}$  crystals with  $x \geq 11.5$  [11].

In the case of a DW instability, theory predicts the existence of phase and amplitude collective modes of the DW order parameter [12]. The amplitude excitation is Raman active and the phase mode should be seen in optical absorption [12,13]. In an ideal system the current carrying phase mode can slide without friction [14], while impurities or lattice commensurability destroy the infinite conductivity and shift this mode to finite frequency as has been experimentally observed [13,15]. In addition, many well established DW compounds display a loss peak that has strongly temperature dependent energy and damping relating to the  $dc$  conductivity of the material [16]. This screened longitudinal excitation has been observed in the transverse response by measurements of the complex finite frequency dielectric constant  $\epsilon(\omega)$ . Electronic Raman scattering can probe the longitudinal electronic channel, essentially the response of the charge density because the Raman response function  $\chi''(\omega) \propto \text{Im}(1/\epsilon(\omega))$  [17]. The existence of collective DW excitations is clearly established for  $\text{Sr}_{14}\text{Cu}_{24}\text{O}_{41}$  [18] by measurements of non-linear conduction and the relaxational dielectric response in the  $10 - 10^6 \text{ Hz}$  region displaying a scattering rate that scales with the  $dc$  conductivity.

One important question is what are the Raman signatures of these collective modes and whether DW correlations still persist at higher carrier dopings in ladder systems. Here we present low frequency Raman scattering results that reveal longitudinal (screened) collective charge density oscillations between  $250$  and  $650 \text{ K}$  in  $\text{Sr}_{14-x}\text{Ca}_x\text{Cu}_{24}\text{O}_{41}$  crystals within a wide concentration range,  $0 < x < 12$ . The characteristic quasi-elastic scattering peak (QEP) we observed in the  $1.5 - 8 \text{ cm}^{-1}$  range above  $300 \text{ K}$  softens with cooling and is present only for polarization parallel the ladder direction. A hy-

hydrodynamic model [19] quantitatively accounts for the collective excitations seen in the Raman response for  $\text{Sr}_{14}\text{Cu}_{24}\text{O}_{41}$  compound. The presence of the QEP in  $\text{Sr}_2\text{Ca}_{12}\text{Cu}_{24}\text{O}_{41}$  demonstrates that density wave correlations are present, at least for temperatures above 250 K, even in superconducting (under pressure) crystals.

We measured Raman scattering from freshly cleaved *ac* surfaces of  $\text{Sr}_{14-x}\text{Ca}_x\text{Cu}_{24}\text{O}_{41}$  and  $\text{La}_6\text{Ca}_8\text{Cu}_{24}\text{O}_{41}$  single crystals grown as described in [6,9]. Excitation energies of 1.55 and 1.65 eV from a  $\text{Kr}^+$  laser were used. The spectra were taken using a custom triple grating spectrometer and corrected for the spectral response of the spectrometer and detector. For measurements below  $T = 300$  K the samples were mounted in a continuous flow optical cryostat and for above room temperature in a TS1500 Linkam heat stage. Stokes and anti-Stokes spectra were taken for all data above 300 K to determine the temperature in the laser spot.

Fig. 1 shows temperature dependent Raman spectra for  $\text{Sr}_{14}\text{Cu}_{24}\text{O}_{41}$  and  $\text{Sr}_2\text{Ca}_{12}\text{Cu}_{24}\text{O}_{41}$  in *cc* polarization. The low frequency Raman spectra at high temperatures in both crystals look qualitatively similar. They are dominated by the presence of strong quasi-elastic scattering rising from the lowest measured energy of about  $1.5 \text{ cm}^{-1}$  and peaked about  $7 \text{ cm}^{-1}$  for temperatures around 620 K. With cooling the QEP shifts to lower frequencies and it gains spectral weight. Below  $T \approx 450$  K the peak position moves below the instrumental cut-off energy and only the high frequency tail of the peak is observed.

The polarization dependence of the QEP are summarized in Fig. 2. For  $\text{Sr}_{14}\text{Cu}_{24}\text{O}_{41}$  (Fig. 2a) the QEP is present in *cc* and absent in *aa* polarization. We do not observe the QEP in *cc* polarization for  $\text{La}_6\text{Ca}_8\text{Cu}_{24}\text{O}_{41}$  (Fig. 2b) which contains no holes per formula unit. The presence of quasi-elastic scattering for  $x > 0$   $\text{Sr}_{14-x}\text{Ca}_x\text{Cu}_{24}\text{O}_{41}$  exhibiting the same polarization selection rules as shown in panels *c* and *d* of Fig. 2 proves that this feature is a characteristic of these compounds at all Ca substitution levels. Applied magnetic fields up to 8 T influenced neither the energy of the QEP nor the modes seen in Fig. 2a and b at  $12 \text{ cm}^{-1}$  in  $\text{Sr}_{14}\text{Cu}_{24}\text{O}_{41}$  and about  $15 \text{ cm}^{-1}$  in  $\text{La}_6\text{Ca}_8\text{Cu}_{24}\text{O}_{41}$ . We can conclude that the latter features are phonons. The unusually low energy of these modes which points towards a very high effective mass oscillator is interesting. These 'folded' phonons appear as a result of chain-ladder incommensurability [4] that gives rise to a big unit cell.

The inset in Fig. 1 shows a typical deconvolution of the Raman data by a fit to a relaxational form:

$$\chi''(\omega) = A(T) \frac{\omega\Gamma}{\omega^2 + \Gamma^2}. \quad (1)$$

A second phenomenological term accounting for a small underlying electronic background was also used. The temperature dependent fitting parameters are shown in

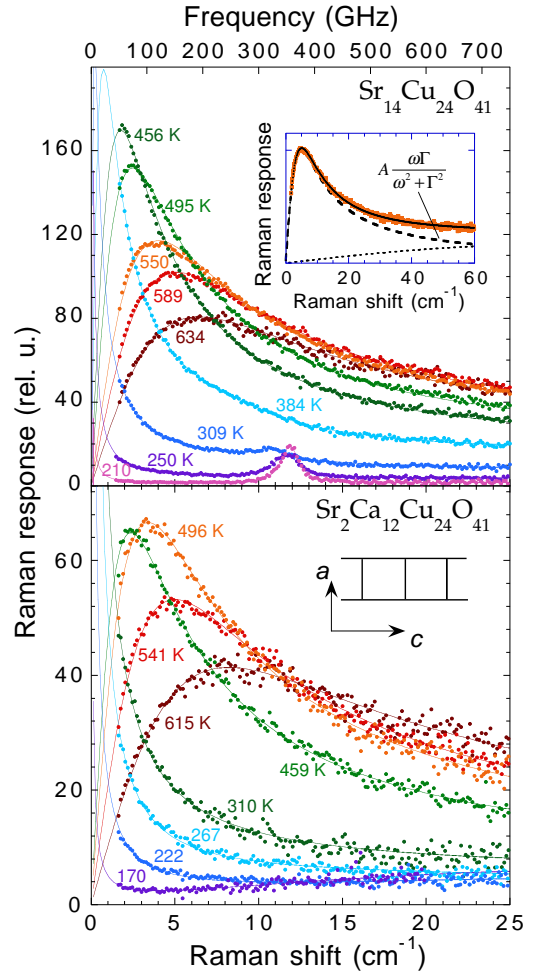


FIG. 1. Temperature dependent Raman response for *cc* polarization in  $\text{Sr}_{14}\text{Cu}_{24}\text{O}_{41}$  and  $\text{Sr}_2\text{Ca}_{12}\text{Cu}_{24}\text{O}_{41}$  taken with the 1.55 eV excitation energy. Upper inset: Typical fit of the Raman data with a relaxational form, Eq. (1), and a small contribution from an underlying background. For temperatures below 310 K the fits for  $\text{Sr}_{14}\text{Cu}_{24}\text{O}_{41}$  included also the phonon around  $12 \text{ cm}^{-1}$ . Lower inset: Two-leg ladder structure and axes notation.

the Fig. 3. An Arrhenius plot for the damping parameter  $\Gamma$  reveals an activated behavior of the form  $\Gamma(T) \propto \exp(-\Delta/T)$  with  $\Delta \approx 2100$  K and 2180 K for  $\text{Sr}_{14}\text{Cu}_{24}\text{O}_{41}$  and  $\text{Sr}_2\text{Ca}_{12}\text{Cu}_{24}\text{O}_{41}$  respectively. These energies are very close to the activation energy displayed by the *c* axis *dc* conductivity for  $\text{Sr}_{14}\text{Cu}_{24}\text{O}_{41}$  crystal [9,20] shown in the inset of Fig. 3. The Raman QEP traces to high temperatures the relaxational peak seen in transport [18], suggesting their common origin. Also, the frequency of the QEP, which is much lower than the thermal energy, the magnetic or *dc* activation gaps, points toward a collective rather than a single particle excitation. For  $\text{Sr}_2\text{Ca}_{12}\text{Cu}_{24}\text{O}_{41}$  the QEP is also present (Fig. 1b). The relaxation parameter  $\Gamma$  is slightly higher than for  $\text{Sr}_{14}\text{Cu}_{24}\text{O}_{41}$  sample while the spectral weight is lower. However, for  $\text{Sr}_2\text{Ca}_{12}\text{Cu}_{24}\text{O}_{41}$  the *c*-axis *dc* conductivity

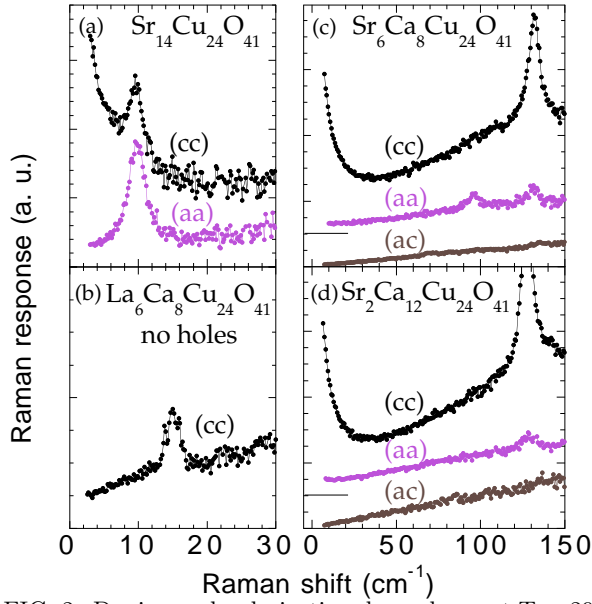


FIG. 2. Doping and polarization dependence at  $T = 295$  K of the quasielastic scattering peak (QEP) in spectra taken with 1.65 eV excitation. (a) For  $\text{Sr}_{14}\text{Cu}_{24}\text{O}_{41}$  the QEP is present in *cc* and absent in *aa* polarizations. (b) For  $\text{La}_6\text{Ca}_8\text{Cu}_{24}\text{O}_{41}$  the QEP is not present. In panels (c) and (d) we observe the QEP for  $x = 8$  and  $12$   $\text{Sr}_{14-x}\text{Ca}_x\text{Cu}_{24}\text{O}_{41}$  only in *cc* polarization. The *aa* data is offset.

above  $T \approx 70$  K shows a metallic behavior.

In the analysis of the Raman spectra shown in Fig. 1 we interpret the low frequency overdamped excitation as a DW relaxational mode in the longitudinal channel. The interaction of longitudinal DW modes with normal (uncondensed) carriers resembles to some degree the problem of coupling of plasma oscillations to the longitudinal optical (LO) vibrations in doped semiconductors [21]. The longitudinal modes of one excitation interact with the electrostatic field produced by the other and as result their bare energy gets renormalized due to screening effects. Essentially a feature which should be observed only in the longitudinal channel, the DW mode leaks into the transverse response due to the non-uniform pinning which introduces disorder mixing the pure transverse and longitudinal character of the excitations [19]. This was seen for  $\text{Sr}_{14}\text{Cu}_{24}\text{O}_{41}$  [18] as well as for other DW compounds [16]. Modelling the DW contribution to the dielectric function by an oscillator, we have:

$$\epsilon_{DW}(\omega) = \frac{\Omega_p^2}{\omega^2 - i\gamma_0\omega - \Omega_0^2}. \quad (2)$$

where  $\Omega_0$  is the characteristic pinning frequency,  $\gamma_0$  an intrinsic damping coefficient and  $\Omega_p^2 = 4\pi\rho_c^2/m^*$  is the spectral weight of the DW given in terms of  $\rho_c$  and  $m^*$  which are the associated charge and effective mass densities. A more realistic model would allow for a broad distribution of pinning frequencies, extending over several decades, as inferred from the low frequency response

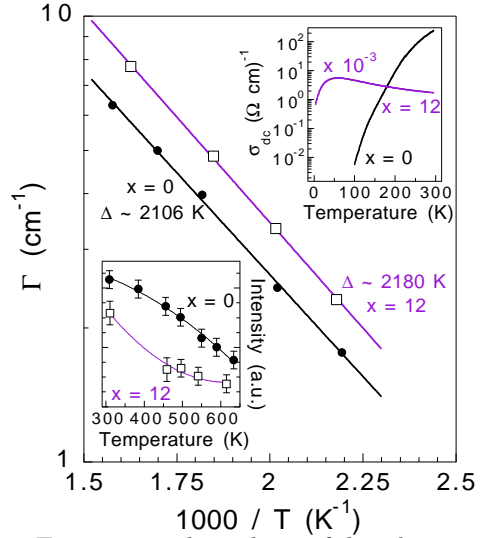


FIG. 3. Temperature dependence of the relaxational rate  $\Gamma$  for  $\text{Sr}_{14}\text{Cu}_{24}\text{O}_{41}$  (filled circles) and  $\text{Sr}_2\text{Ca}_{12}\text{Cu}_{24}\text{O}_{41}$  (empty squares). An activated behavior  $\Gamma \propto \exp(-\Delta/T)$  is observed for both compounds. Upper inset: Temperature dependence of the *dc* conductivity as a function of temperature. Note that the data for  $\text{Sr}_2\text{Ca}_{12}\text{Cu}_{24}\text{O}_{41}$  was divided by a factor of  $10^3$ . Lower inset: Variation of the quasi-elastic peak weight,  $A(T)$ , with temperature (solid lines are guides for the eye).

[16,18]. Within a two-fluid model, assuming that the only coupling between condensed and normal electrons is by an electric field due to density fluctuations, the longitudinal response which accounts for the screening effects and is relevant for Raman scattering can be written as [19]:

$$\epsilon_L = \frac{\Omega_p^2}{\Omega_0^2 - \omega^2 - i\gamma_0\omega - \frac{i\omega\Omega_p^2}{4\pi\sigma_{dc} - i\omega\epsilon_\infty}} \quad (3)$$

Here  $\sigma_{dc}$  is the 'quasiparticle' conductivity and  $\epsilon_\infty$  takes into account the contribution of high frequency interband transitions to the polarization. Note that in the low frequency limit, Eq. (3) reduces to the relaxational form of Eq. (1), with a weight  $A(T) = \Omega_p^2/\Omega_0^2$  and a damping

$$\Gamma(T) = 4\pi\sigma_{dc}\Omega_0^2/\Omega_p^2. \quad (4)$$

The proportionality between  $\Gamma$  and the *dc* conductivity, which is clearly seen in Fig. 3 for  $\text{Sr}_{14}\text{Cu}_{24}\text{O}_{41}$ , is the result of normal carrier backflow which screens the collective polarization and dissipates energy, suffering lattice momentum relaxation [19].

Extrapolating the activated fit for the conductivity in between 150 and 300 K for  $\text{Sr}_{14}\text{Cu}_{24}\text{O}_{41}$  to temperatures higher than 450 K, where the QEP was still seen in Raman spectra, we calculated the values for  $\Gamma(T)$  from Eq. (4) using  $\Omega_0 \approx 1\text{-}4\text{ cm}^{-1}$  and  $\Omega_p \approx 3300\text{ cm}^{-1}$  as determined from low temperature microwave data [22] and the *c*-axis loss function [23]. This independent calculation yields values which are lower by a factor of 25 than the Raman data suggests. There are two reasons which can

explain this discrepancy. One is related to the reduction in the density of condensed carriers in close proximity to the DW transition. The second is that the distribution of pinning frequencies is in the range of measured Raman shifts, so that we obtain a contribution to a Raman response of the form of Eq. (1) only from the higher part of the distribution. Furthermore, above  $T \approx 150$  K the width of the pinning frequencies distribution increases. Although  $\Omega_0$  might still be centered around  $1\text{--}4\text{ cm}^{-1}$  [22], the mode becomes strongly broadened at high temperatures. Eq. (3) also predicts a charge DW plasmon at the frequency  $(\Omega_0^2 + \Omega_p^2/\epsilon_\infty)^{1/2} \approx 1500\text{ cm}^{-1}$ . We do not observe this feature in our spectra due to the strong damping and the fact that it lies in the midst of a strong multi-phonon scattering region.

For  $\text{Sr}_2\text{Ca}_{12}\text{Cu}_{24}\text{O}_{41}$  above 70 K the *dc* conductivity is metallic [9]. However, the Raman response in the  $2\text{--}8\text{ cm}^{-1}$  region (Fig. 1) is qualitatively similar to the  $\text{Sr}_{14}\text{Cu}_{24}\text{O}_{41}$  crystal. The similarity of the results allows us to conclude that DW correlations are also present at high Ca substitution levels. We propose that the metallic behavior for  $\text{Sr}_2\text{Ca}_{12}\text{Cu}_{24}\text{O}_{41}$  is due to a partially gapped Fermi surface. Support for this conjecture comes from an angle resolved photoemission study [25] which shows that while for  $\text{Sr}_{14}\text{Cu}_{24}\text{O}_{41}$  the gap is finite, for  $\text{Sr}_5\text{Ca}_9\text{Cu}_{24}\text{O}_{41}$  the density of states rises almost to the chemical potential. This spectral weight transfer is enhanced with further increase in the ladder hole concentration [6]. The observation of an activated relaxation rate in the metallic  $x = 12$  compound is not consistent with Eq. (3), based on a simple two-fluid assumption. Note however that by room temperature the  $x = 0$  and  $x = 12$  compounds have comparable conductivities, suggesting that the contribution of the remnant Fermi surface to the overall carrier density is quite small. Similar relaxation rates for  $\text{Sr}_{14}\text{Cu}_{24}\text{O}_{41}$  and  $\text{Sr}_2\text{Ca}_{12}\text{Cu}_{24}\text{O}_{41}$  might be reconciled with different transport properties assuming a strongly momentum dependent scattering rate. Carrier condensation in the DW state leads to a completely gapped Fermi surface resulting in an insulating behavior below  $T = 70$  K. In addition, the DW dynamics in  $\text{Sr}_2\text{Ca}_{12}\text{Cu}_{24}\text{O}_{41}$  is influenced by the random potential introduced in the system because of cation substitution which affects the pinning mechanism [24]. Another more speculative explanation for the metallic like conductivity in  $\text{Sr}_2\text{Ca}_{12}\text{Cu}_{24}\text{O}_{41}$  could be that in the presence of a very broad distribution of pinning frequencies  $\Omega_0$  as a result of Ca substitution, not all the collective contribution gets pinned, and we still have a Fröhlich type component [14] contributing to the *dc* conductivity. Irrespective of the exact microscopic model, strong similarities between local structural units and transport properties in Cu-O based ladders and underdoped high  $T_c$  materials suggest that carrier dynamics in 2D Cu-O sheets at low hole concentration could be also governed by a collective DW response.

In conclusion we demonstrated the existence of DW correlations in doped two-leg  $\text{Sr}_{14-x}\text{Ca}_x\text{Cu}_{24}\text{O}_{41}$  ladders. We found Raman fingerprints of screened longitudinal collective modes in crystals with Ca concentrations from  $x = 0$  to 12. A hydrodynamic model was used to quantitatively account for the existence of the charge collective mode in the insulating  $\text{Sr}_{14}\text{Cu}_{24}\text{O}_{41}$  compound whose damping scales with the activated conductivity. This mode is also present in the superconducting (under pressure)  $\text{Sr}_2\text{Ca}_{12}\text{Cu}_{24}\text{O}_{41}$  ladder. Our results demonstrate that the paired superconducting state competes in these materials with a crystalline charge ordered ground state.

---

<sup>†</sup> To whom correspondence should be addressed. E-mail: girsh@bell-labs.com

- [1] S. Sachdev, *Science* **288**, 475 (2000).
- [2] E. Dagotto and T. M. Rice, *Science* **271**, 618 (1996); E. Dagotto, *Rep. Prog. Phys.* **62**, 1525 (1999) and references therein.
- [3] E. Dagotto, J. Riera, and D. Scalapino, *Phys. Rev. B* **45**, 5744 (1992); T. M. Rice, S. Gopalan, and M. Sigrist, *Europhys. Lett.* **23**, 445 (1993).
- [4] E. M. McCarron III *et al.*, *Mater. Res. Bull.* **23**, 1355 (1988); T. Siegrist *et al.*, *Mater. Res. Bull.* **23**, 1429 (1988).
- [5] M. Kato *et al.*, *Physica C* **258**, 284 (1996).
- [6] T. Osafune *et al.*, *Phys. Rev. Lett.* **78**, 1980 (1997).
- [7] T. Osafune *et al.*, *Phys. Rev. Lett.* **82**, 1313 (1999).
- [8] J. Vanacken *et al.*, *Physica C* **337**, 260 (2000).
- [9] N. Motoyama *et al.*, *Phys. Rev. B* **55**, R3386 (1997).
- [10] Y. Ando *et al.*, *Phys. Rev. Lett.* **87**, 017001 (2001).
- [11] M. Uehara *et al.*, *J. Phys. Soc. Jpn.* **65**, 2764 (1996); T. Nagata *et al.*, *Phys. Rev. Lett.* **81**, 1090 (1998).
- [12] P. A. Lee, T. M. Rice, and P. W. Anderson, *Solid State Comm.* **14**, 703 (1974).
- [13] G. Grüner, *Density waves in solids* (Perseus publishing, Cambridge, Massachusetts, 1994).
- [14] F. R. S. Fröhlich, *Proc. R. Soc., Lond.* **A223**, 296 (1954).
- [15] L. Degiorgi *et al.*, *Phys. Rev. B* **44**, 7808 (1991) and references therein.
- [16] W. Wu *et al.*, *Phys. Rev. Lett.* **52**, 2382 (1984); R. J. Cava *et al.*, *Phys. Rev. B* **33**, 2439 (1986); **30**, 3228 (1984).
- [17] M. V. Klein, Chap. 4 in *Light Scattering in Solids I*, (Ed. M. Cardona, Springer-Verlag, 1983).
- [18] G. Blumberg *et al.*, *Science* **297**, 26 July (2002).
- [19] P. B. Littlewood, *Phys. Rev. B* **36**, 3108 (1987).
- [20] M. W. McElfresh *et al.*, *Phys. Rev. B* **40**, 825 (1989).
- [21] I. Yokota, *J. Phys. Soc. Jpn.* **16**, 2075 (1961).
- [22] H. Kitano *et al.*, *Europhys. Lett.* **56**, 434 (2001).
- [23] H. Eisaki *et al.*, *Physica C* **341-348**, 363 (2000).
- [24] L. F. Schneemeyer *et al.*, *Phys. Rev. B* **30**, 4297 (1984).
- [25] T. Takahashi *et al.*, *Phys. Rev. B* **56**, 7870 (1997).